Dielectronic Resonance Method for Measuring Isotope Shifts

R. Schuch,[1,†] E. Lindroth,[1] S. Madzunkov,[1] M. Fogle,[1] T. Mohamed,[1] and P. Indelicato[2]

[1]*Atomic Physics, Stockholm University, AlbaNova, S-106 91 Stockholm, Sweden*

[2]*Laboratoire Kastler Brossel*, École Normale Supérieure et Université Pierre et Marie Curie, Case 74, 4 place Jussieu, F-75252, Cedex 05, France*

(Received 28 February 2005; published 28 October 2005)

Long standing problems in the comparison of very accurate hyperfine-shift measurements to theory were partly overcome by precise measurements on few-electron highly charged ions. Still the agreement between theory and experiment is unsatisfactory. In this Letter, we present a radically new way of precisely measuring hyperfine shifts, and demonstrate its effectiveness in the case of the hyperfine shift of $4s_{1/2}$ and $4p_{1/2}$ in $^{207}Pb^{53+}$. It is based on the precise detection of dielectronic resonances that occur in electron-ion recombination at very low energy. This allows us to determine the hyperfine constant to around 0.6 meV accuracy which is on the order of 10%.

DOI: 10.1103/PhysRevLett.95.183003 PACS numbers: 31.30.Gs, 31.30.Jv, 34.80.Lx

The hyperfine structure (hfs) in atoms reflects fundamental high-order effects in the interaction between the bound electrons and the nucleus. The energy shift contains contributions from quantum electrodynamics (QED) and from the nuclear charge and magnetic-moment distribution [1]. These effects have been studied over decades by spectroscopy, mainly on neutral atoms or singly charged ions. In such many-electron systems, the atomic structure is complex. The theoretical predictions are further hampered by imprecise knowledge of nuclear magnetic moments which, if measured in a magnetic field, are shielded due to diamagnetic effects [1], which can only be estimated and corrected for through calculations. Only recently have experimental approaches to measure the hyperfine structure of heavy highly charged systems been opened [2–5], giving a new way to obtain nuclear moments and to test QED in a new regime. Measurements were done for several hydrogenlike ions: $^{209}Bi^{82+}$, $^{165}Ho^{66+}$, $^{183\,187}Re^{74+}$, $^{203\,205}Tl^{80+}$, and $^{207}Pb^{81+}$ [2–5]. In all cases the theory and experiment do not agree in a satisfactory way. The largest theoretical uncertainty comes from the unknown distribution of nuclear magnetic moments (Bohr-Weisskopf effect), which is complicated to predict due to nuclear polarization [6], but also precise knowledge of the charge radius is crucial. On the other hand, a determination of nuclear magnetic-moment distribution is impossible due to uncertainties in the QED prediction. Although the measurements with H-like ions are quite accurate (2×10^{-4} for ^{207}Pb [4]), it is still essential to find alternative approaches to measure hyperfine structure for different ion charges where the above mentioned effects contribute differently.

Here we demonstrate a first measurement of the hyperfine structure in ^{207}Pb by observing dielectronic recombination (DR) resonances for both $^{208}Pb^{53+}$ (zero nuclear spin) and $^{207}Pb^{53+}$ (nuclear spin one-half). Using the two Pb isotopes in charge state 53+, one clearly observes hyperfine effects in $4s_{1/2}$ and $4p_{1/2}$ $F = 1$ and $F = 0$ states. The importance of this observation is that it provides means to easily measure the hyperfine interaction of $^{207}Pb^{53+}$, and other ions with a different number of electrons, as compared to what is currently possible. By measuring the same nucleus with different numbers of electrons one can measure their influence on the magnetic interaction and check the theories including QED and probably do even better by extrapolating to low electron numbers. A similar idea, combining the $1s$ hyperfine shift in H-like and the $2s$ shift in Li-like ions to extract QED contributions, was recently proposed in a theoretical paper [7]. A further application of this method can be found in the new accumulator rings for radioactive nuclei to measure their nuclear magnetic properties by low-energy electron scattering in the cooler [8].

The spectroscopic principle of using DR resonances is that the valence electron is excited by the capture of a free electron into a Rydberg state. The measured resonances are near threshold, thus the Rydberg energy must balance to a large part the excitation energy of the valence electron. Higher order effects in the interaction of the Rydberg electron with the core electrons are weak and can be estimated to excellent accuracy. The measurement is checked by comparing the DR resonances with those of $^{208}Pb^{53+}$ where no hyperfine splitting exists. In the $^{208}Pb^{53+}$ case we previously reached an accuracy that enabled us to obtain spectroscopic data for stringent tests of many-electron QED effects in advanced atomic structure calculations [9].

Selected ^{207}Pb or ^{208}Pb isotopes are injected as singly charged ions from an isotope separator, at the Manne Siegbahn Laboratory in Stockholm, into an electron-beam ion source, where the highly charged Pb ions are created. From there they are injected into the heavy-ion storage ring CRYRING, and accelerated to several MeV/amu. After electron cooling the ion beam for 1 s, the recombination rates as a function of relative energy between electrons and ions are measured. This is achieved

by ramping the electron energy up and down, from the cooling condition to a maximum energy in the center-of-mass frame, so that recombination spectra are obtained both with the electrons being slower and faster than the ions. Thus, we can check the space charge of the electron beam and the longitudinal drag force exerted on the ions by the electrons during detuning and make appropriate corrections [10,11]. These corrections are important in order to obtain accurate energy scales in the spectra. The energy calibration was checked thoroughly and found to be accurate to within 0.1 meV at energies ≤ 0.3 eV. For these low energies one takes full advantage of the small energy spread of the adiabatically expanded electron beam [12] and obtains a resolution on the order of 1 meV. From fits to the resonances, we confirm the longitudinal and transversal temperatures of the electron beam to be $kT_l = 0.1$ meV and $kT_t = 2$ meV, respectively.

The consistency of the measurement is checked by switching between the $^{207}Pb^{53+}$ and $^{208}Pb^{53+}$ beams. Small changes in the magnet field strengths were made for the two isotope ions to have the same velocity (determined by electron cooling) and the same circulation frequency in the ring (measured by the Schottky frequency). We also compare the $^{208}Pb^{53+}$ data measured in this run with those measured earlier (with $kT_l = 0.08$ meV and $kT_t = 1$ meV) and published in Ref. [9] (see Fig. 1). Considering the small temperature difference, these data sets agree within the statistical error (its size is seen in the spread of the points). In Fig. 1 we also show the recombination rate coefficient that was obtained with $^{207}Pb^{53+}$ stored in the ring. The difference between the two sets of experimental spectra must then be due to the isotope effect, in particular, the hyperfine shifts of the $F = 0$ and 1 states in $4s_{1/2}$ and $4p_{1/2}$ of $^{207}Pb^{53+}$.

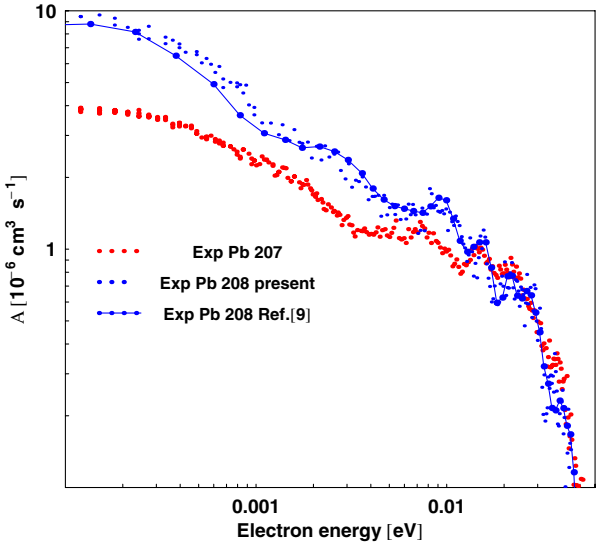

FIG. 1 (color online). Measured dielectronic recombination spectra with $^{207}Pb^{53+}$ and with $^{208}Pb^{53+}$.

We have evaluated the isotope dependent contributions to Pb^{53+} $(4\ell_{1/2})$ using both relativistic many-body perturbation theory (RMBPT) [13] and a multi-configuration Dirac-Fock (MCDF) computer package [14,15]. We have carefully checked the agreement between the methods. The dominating effect, listed in detail on the first six lines of Table I, is due to the coupling between the total electronic angular momentum and the nuclear magnetic moment of the spin one-half ^{207}Pb nucleus. Most of the contribution is accounted for already with a single-configuration DF calculation using a point nucleus, as seen on the first line. The lead wave function has then been evaluated in a potential from an extended nucleus, which results in a $\sim 10\%$ change in the $4s$ hyperfine structure, as seen on the second line of Table I. We use a Fermi distribution of the nuclear charge with thickness parameter 2.3 fm and a half density radius adjusted to produce a charge root mean square radius (rms) of 5.4942(0.0013) fm [17]. The wave function has also been allowed to adjust to the Breit interaction between the electrons and to the Uehling potential (responsible for the bulk of the vacuum polarization), but the effect on the hyperfine structure is very small. All these contributions agree within the displayed digits between the two computational methods. The polarization of the closed shell core by the valence electron give rise to important corrections to the hyperfine structure. These effects can only be accounted for when spherical symmetry is abandoned, but they are still not true correlation effects. We have calculated this core polarization using RMBPT (fourth line). The dominating part of the core polarization is accounted for already in second order (one order in the hyperfine structure and one order in the Coulomb interaction). The results change with only a few μeV when higher order core polarization is taken into account. Since it is also true that

TABLE I. Binding energy of $^{207}Pb^{53+}(4j_{1/2})$ relative the $(4j_{1/2})$ states in $^{208}Pb^{53+}$ (meV).

	$4s_{1/2}$		$4p_{1/2}$	
	$F=0$	$F=1$	$F=0$	$F=1$
Contributions $\sim\mu_I$[a]				
point size μ_I				
Dirac-Fock point nucleus	−12.16	4.05	−3.66	1.22
Δ nuclear size	1.37	−0.46	0.12	−0.04
Δ Breit and Vac. pol.	−0.03	0.01	0.03	−0.01
Δ core polarization[b]	−0.34	0.11	−0.12	0.04
Δ correlation	−0.03	0.01	0.04	−0.01
distributed μ_I	0.23	−0.08	0.02	−0.01
(Bohr-Weisskopf effect)				
Sum	−10.97	3.66	−3.57	1.19
Contributions independent of μ_I	−1.59	−1.59	−0.08	−0.08
(Volume shift)				
Total	−12.56	2.06	−3.65	1.11

[a] $\mu_I/\mu_N = 0.5918$, Ref. [16].
[b] Includes polarization due to both the Coulomb and the Breit interaction, the latter contributes with 10–14%.

correlation, calculated with either RMBPT or MCDF, gives negligible contributions (see Table I) it is evident that the many-body aspect of Pb^{53+} does not limit the potential accuracy of the determination of the hyperfine structure. An approximate Bohr-Weisskopf effect is included, assuming the same mean spherical radius for the magnetic-moment distribution as was used for the charge distribution, following, e.g., Ref. [15]. Also here the two computational methods agree to within one unit in the last quoted digit.

An additional isotope dependent contribution originates from the slightly different potentials produced by nuclei with different rms (volume shift). According to Angeli [17] the rms of ^{207}Pb is 0.0068(0.0002) fm smaller than that of ^{208}Pb. This leads to $\sim$1.6 meV larger binding energy for the $4s$ state of ^{207}Pb, corresponding to $\sim 0.2\ \mathrm{meV}/10^{-3}$ fm, as seen in Table I.

The experimental evaluations of the magnetic moment of, e.g., ^{207}Pb, have been critically evaluated in Ref. [1], indicating that the true value should be within error bars of the atomic beam magnetic resonance result by Brenner $\mu_I = 0.5918(14)\mu_N$ [16] and the NMR result by Lutz and Stricker [18], quoted in Ref. [1] as $\mu_I = 0.5925(6)\mu_N$. While the optical pumping result by Gibbs and White [19], which is $\approx 1.3\%$ below Ref. [16], seems to suffer from systematic errors. Here we have used the value from Ref. [16].

As in ^{208}Pb [9] the recombination goes through resonances in Pb^{52+}, $Pb^{53+}(3d^{10}4s_{1/2}) + e^- \rightarrow Pb^{52+}(3d^{10}4p_{1/2}18\ell_j)_J$. The term splitting of these excited states range from a few meV for the states around the ionization threshold, $j = 21/2$, of $^{208}Pb^{52+}$ [9] to practically zero for the highest angular momenta. When considering hyperfine structure we note first that the J- dependent term splitting and the hyperfine splitting of the $4p_{1/2}$ orbital energy are of the same order of magnitude. The energy levels are then expected to be governed by intermediate coupling and will not scale linearly with the hyperfine shift; each level will be an individual mix of the two hyperfine components of the inner electron orbital. The hyperfine interaction involving the outer $18\ell_j$ electron will be much smaller due to the $1/n^3$ scaling of the radial matrix elements and will be neglected in the following. Starting from the $(4p_{1/2}18\ell_j)_J$ energy levels in the absence of hyperfine interaction [9], using the assumption that only terms (J) belonging to the same configuration will mix due to the hyperfine interaction, and using the knowledge of the splitting of the $4p_{1/2}$ in the absence of the Rydberg electron, it is straightforward to generate the hyperfine perturbed resonance energies with standard angular momentum theory. Without hyperfine interaction each $4p_{1/2}18\ell_j$ configuration forms two J terms. With hyperfine interaction we get four energy levels of which two mix the J terms. The recombination cross section can now be constructed from the energy positions relative the initial state of Pb^{53+}, the autoionization rates, and the stabilizing radiative rates to bound states of Pb^{52+}. The autoionization rate varies strongly and is governed by the actual mixture just discussed. The radiative rate is for these high angular momenta states dominated by the probability for the $4p \rightarrow 4s$ transition and is thus slowly varying and nearly constant for all the investigated resonances. The position of a resonance is affected by the positions of the hyperfine perturbed excited states as well as of the shifted initial state. The ground state of $Pb^{53+}4s$ is with hyperfine interaction split into one state with $F = 0$ and one with $F = 1$. The $F = 1$ state has higher energy, but its decay to $F = 0$ is very slow. The expected lifetime is 2.3×10^4 s [7] which is much longer than the time from ions production to the measurement ($\sim$5 s). We have thus assumed a statistical population of the two $Pb^{53+}(4s_{1/2})_F$ states and the recombination cross section from the two possible initial states have been calculated and added with statistical weights. This cross section has subsequently been folded with the electron-beam velocity distribution mentioned above.

The nuclear spin dependent part of the hyperfine energy shift is $\Delta E_{\mathrm{hfs}} = a/2[F(F+1) - I(I+1) - J(J+1)]$, where a is the hyperfine splitting constant for a given state, J is the electronic angular momentum, I is the nuclear spin, and F is the total angular momentum. Using the fact that $3a_{4p} \approx a_{4s}$ to within 2–3%, as shown in Table I, we generate a synthetic spectrum derived from the resonance parameters as described above, and test the sensitivity with respect to small variations in $a = a_{4p}$. The theoretical shifts in Table I are approximately reproduced by $a = 4.8$ meV. Figure 2 shows the spectrum generated with the theoretical shifts as well as with a values deviating

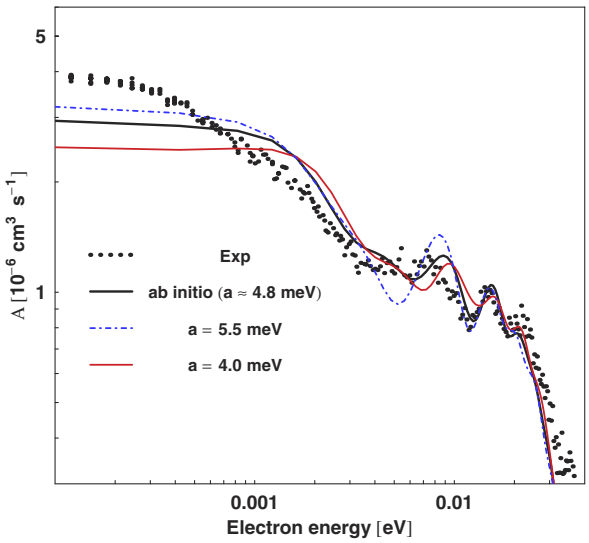

FIG. 2 (color online). Recombination rate coefficients A for $^{207}Pb^{53+}$, the calculated ones are with different values of the hyperfine constant, a, as explained in the text. The comparison is absolute, both in energy and in A.

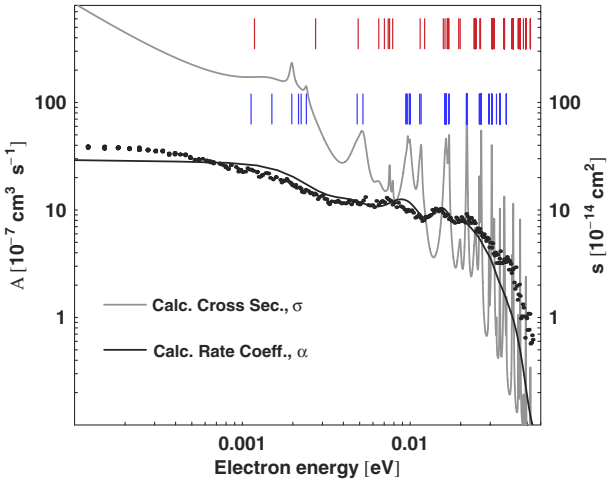

FIG. 3 (color online). Calculated resonance positions for initial states $^{207}Pb^{53+}(4s_{1/2})_{F=0}$, upper sequence of levels, and $^{207}Pb^{53+}(4s_{1/2})_{F=1}$, lower sequence of levels. The gray line shows the cross section s assuming statistical population of these two hyperfine structure components. From this cross section the rate coefficient, the black solid line, is generated. It should be compared to the measured rate coefficient for $^{207}Pb^{53+}$, shown as black dots.

from it with around ± 0.7 meV. The spectrum generated from the calculated shifts seems to fit the data best. Note that different peaks in the spectrum are rather differently affected when a is changed, reflecting the nonlinear shift of the resonances. With $a = 5.5$ meV the synthetic spectrum shows much more pronounced resonances and with $a = 4.0$ meV the dip around 0.01 eV has nearly disappeared. We estimate from this procedure that with the present energy spread of the electron beam we can get an accuracy in determining a, from a fit to the resonances, to the order of ± 0.3 meV. Here the statistical error was taken into account. With a specially designed electron target of lower energy spread, one could reduce the uncertainty further. Figure 3 shows the positions of all the resonances and the cross section before folding with the electron temperature.

At the present stage we are also limited in our accuracy by the uncertainty in describing the resonances. This problem already exists in the $^{208}Pb^{53+}$ case [9]. There is a so far unexplained discrepancy between theory and measured rate coefficient at energies below 1 meV. That may cause the systematic uncertainty to reach 1 meV. Several resonances above 1 meV are well described by the calculated series. Another unexplained discrepancy appears at energies larger than 0.03 eV (see Fig. 3). As can be seen from Fig. 3 the highest energy resonances contribute insignificantly to the cross section. The reason might be that the autoionization rates approach zero for these high angular momenta states, but even small electromagnetic fields in the cooler could change this by inducing a mixture with states of low angular momentum. This possibility has to be investigated further, but will not affect the conclusions here since in this range one is not very sensitive to a hyperfine splitting in the order of meV.

In conclusion, the hyperfine splittings in $4p_{1/2}$ and $4s_{1/2}$ state of the Cu-like ^{207}Pb isotope were measured by a new method to an accuracy of the order 10% of the hfs constant. Instead of the generally applied optical spectroscopy, the splitting was observed in dielectronic resonances in low-energy electron-ion recombination. This opens new possibilities to measure this important physical quantity in a new energy range and ionization stage for determining the different contribution to its value.

We thank the CRYRING crew for the skillful operation of the storage ring. We acknowledge support from the Swedish research council (V. R.).

*Laboratoire Kastler Brossel is Unité Mixte de Recherche du CNRS No. 8552.
†Email address: schuch@physto.se

[1] M. G. H. Gustavsson and A.-M. Mårtensson-Pendrill, Phys. Rev. A **58**, 3611 (1998).
[2] I. Klaft *et al.*, Phys. Rev. Lett. **73**, 2425 (1994).
[3] J. R. Crespo López-Urrutia *et al.*, Phys. Rev. Lett. **77**, 826 (1996).
[4] P. Seelig *et al.*, Phys. Rev. Lett. **81**, 4824 (1998).
[5] P. Beiersdorfer *et al.*, Nucl. Instrum. Methods Phys. Res., Sect. B **205**, 62 (2003).
[6] M. Tomaselli *et al.*, Phys. Rev. C **58**, 1524 (1998).
[7] V. M. Shabaev *et al.*, Phys. Rev. A **57**, 149 (1998).
[8] *International Accelerator Facility for Beams of Ions and Anti-Protons*, edited by W. F. Henning (GSI Darmstadt, Germany, 2001), http://www.gsi.de/GSI-future/cdr/; R. Schuch and T. Stoehlker (to be published).
[9] E. Lindroth *et al.*, Phys. Rev. Lett. **86**, 5027 (2001).
[10] W. Zong *et al.*, Phys. Rev. A **56**, 386 (1997).
[11] S. Madzunkov *et al.*, Phys. Rev. A **65**, 032505 (2002).
[12] H. Danared *et al.*, Nucl. Instrum. Methods Phys. Res., Sect. A **441**, 123 (2000).
[13] A.-M. Mårtensson-Pendrill and A. Ynnerman, Phys. Scr. **41**, 329 (1990).
[14] J. P. Desclaux, *A Relativistic Multiconfiguration Dirac-Fock Package*, in Methods and Techniques in Computational Chemistry edited by E. Clementi (STEF, Cagliari, 1993).
[15] S. Boucard and P. Indelicato, Eur. Phys. J. D **8**, 59 (2000).
[16] T. Brenner, Ph.D. thesis, Institut für Angewandte Physik, Universität Bonn, 1988.
[17] I. Angeli, At. Data Nucl. Data Tables **87**, 185 (2004).
[18] O. Lutz and G. Stricker, Phys. Lett. **35A**, 397 (1971).
[19] H. M. Gibbs and C. M. White, Phys. Rev. **188**, 180 (1969).